Morphology Control of PbWO 4 Nano and Microcrystals via a Simple, Seedless, and High-Yield Wet Chemical Route

ARTICLE *in* LANGMUIR · FEBRUARY 2004

Impact Factor: 4.46 · DOI: 10.1021/la035578b

2 AUTHORS:

Xianluo Hu
Huazhong University of Science and Technol…
127 PUBLICATIONS **5,601** CITATIONS
SEE PROFILE

Ying-Jie Zhu
Chinese Academy of Sciences
216 PUBLICATIONS **6,999** CITATIONS
SEE PROFILE

Morphology Control of $PbWO_4$ Nano- and Microcrystals via a Simple, Seedless, and High-Yield Wet Chemical Route

Xian-Luo Hu and Ying-Jie Zhu*

State Key Laboratory of High Performance Ceramics and Superfine Microstructure, Shanghai Institute of Ceramics, Chinese Academy of Sciences, Shanghai 200050, People's Republic of China

Received August 26, 2003. In Final Form: November 28, 2003

Introduction

Currently, controlling the size and dimensionality of nanostructures at the mesoscopic level is one of the most challenging issues faced by researchers.[1−6] Specifically, research on one-dimensional (1D) inorganic nano- and microcrystals has attracted much attention during the past few years because of their fundamental importance in understanding the dependence of properties on the size and dimensionality as well as their novel properties and potential applications in fabricating nanoscale electronic, optoelectronic, and sensing devices.[7−10] Some unique and fascinating properties, such as higher luminescence efficiency, of 1D nanostructures have already been demonstrated.[9] As a result of the quantum confinement effect, 1D nanostructures exhibit distinct optical properties (e.g., the shift of band gap energies) when their diameter approaches a critical value.[11] For example, Korgel and co-workers found that the absorption edge of Si nanowires was significantly blue-shifted as compared with bulk silicon (indirect band gap of ∼1.1 eV) and showed relatively strong "band edge" photoluminescence (PL).[11] Lieber and co-workers reported that there exists a striking anisotropy in PL intensities measured in the direction parallel and perpendicular to the longitudinal axis of an individual InP nanowire.[12] In addition, the Yang group has successfully demonstrated room-temperature ultraviolet lasing from arrays of ZnO nanowires grown on a sapphire substrate.[10]

Recently, nanostructured tungstate materials, such as $CdWO_4$,[13,14] $MnWO_4$,[15] $BaWO_4$,[16−19] $ZnWO_4$,[20] and so forth, have aroused much interest because of their luminescence behavior, structural properties, and potential applications. There have been a number of methods developed to generate nanostructured tungstate materials. For example, $CdWO_4$ nanorods/nanobelts and elongated nanosheets,[13,14] $BaWO_4$ crystals with olivelike, flakelike, and whiskerlike structures,[19] and $ZnWO_4$ nanorods[20] were synthesized via a hydrothermal route. Besides, a solvothermal route for controlling the morphologies of $MnWO_4$ nanocrystals[15] and a reversed micelle templating route for synthesis and assembly of $BaWO_4$ nanorods and nanowires[16−18] were also reported. Lead tungstate ($PbWO_4$) nano- and microcrystals with a tetragonal Scheelite-type structure are of technological importance because of their high density (8.3 g cm^{-1}), short decay time (less than 10 ns for a large part of light output), high-irradiation damage resistance (10^7 rad for undoped and 10^8 rad for La-doped $PbWO_4$), interesting excitonic luminescence, thermoluminescence, and stimulated Raman scatting behavior.[21,22] However, to the best of our knowledge, few studies have been carried out concerning the morphology-controlled synthesis of $PbWO_4$ nano- and microcrystals with various morphologies via a wet chemical route. Herein, we demonstrate a simple, seedless, and high-yield wet chemical route for the synthesis of $PbWO_4$ nano- and microcrystals with various morphologies (rods, spindles, and pagodas). The method involves no seeds, catalysts, or templates and may be scaled up to synthesize $PbWO_4$ nano- and microcrystals on a large scale at relatively low cost.

Experimental Section

Lead acetate [$Pb(CH_3COO)_2{\cdot}3H_2O$], sodium tungstate ($Na_2WO_4{\cdot}2H_2O$), and poly(vinylpyrrolidone) (PVP, $M_W \approx 55\,000$) were of analytical grade and used as received without further purification. In a typical experimental procedure, 20 mL of distilled water was placed in a 100-mL round-bottomed flask and adjusted to the desired pH ∼6.0 by using 2 mol L^{-1} HCl or NaOH. Then, 0.01 mol L^{-1} $Pb(CH_3COO)_2$, 0.01 mol L^{-1} Na_2WO_4, and 0.015 mol L^{-1} PVP (calculated by the repeating unit) were simultaneously injected to the flask just described at room temperature through a three-channel peristaltic pump with a supply rate of ∼0.05 mL min^{-1} for each reactant in a period of 1 h. Vigorous magnetic stirring was continuously applied throughout the entire process of precipitation and crystal growth. After the reactant supply was terminated, the precipitate was left under continuous stirring in its mother solution for 1 (sample 1) to 6 (sample 2) h to ensure complete equilibration or poured into a commercial stainless steel Teflon-lined autoclave of 40-mL capacity (sample 3). The autoclave was maintained at a temperature of 160 °C for 20 h without stirring and shaking during heating and then was allowed to cool to ambient temperature naturally. The products were collected by centrifu-

* Corresponding author: Prof. Ying-Jie Zhu. E-mail: y.j.zhu@mail.sic.ac.cn. Phone: +86-21-52412616. Fax: +86-21-52413122.

(1) Ahmadi, T. S.; Wang, Z. L.; Green, T. C.; Henglein, A.; El-Sayed, M. L. *Science* **1996**, *272*, 1924.
(2) Jana, R.; Gearheart, L.; Murhpy, C. J. *Adv. Mater.* **2001**, *13*, 1389.
(3) Li, L. S.; Hu, J. T.; Yang, W. D.; Alivisatos, A. P. *Nano Lett.* **2001**, *1*, 349.
(4) Sun, Y. G.; Xia, Y. N. *Science* **2002**, *298*, 2176.
(5) Zhu, Y. J.; Hu, X. L. *Chem. Lett.* **2003**, *32*, 732.
(6) Sun, Y. G.; Mayers, B.; Xia, Y. N. *Nano Lett.* **2003**, *3*, 675.
(7) Xia, Y. N.; Yang, P. D.; Sun, Y. G.; Wu, Y. Y.; Mayers, B.; Gates, B.; Yin, Y. D.; Kim, F.; Yan, Y. Q. *Adv. Mater.* **2003**, *15*, 353.
(8) Frank, S.; Poncharal, P.; Wang, Z. L.; de Heer, W. A. *Science* **1998**, *280*, 1744.
(9) Duan, X.; Huang, Y.; Cui, Y.; Wang, J.; Lieber, C. M. *Nature* **2001**, *409*, 66.
(10) Huang, M.; Mao, S.; Feick, H.; Yan, H.; Wu, Y.; Kind, H.; Weber, E.; Russo, R.; Yang, P. *Science* **2001**, *292*, 1897.
(11) Holmes, J. D.; Johnston, K. P.; Doty, R. C.; Korgel, B. A. *Science* **2000**, *287*, 1471 and references therein.
(12) Wang, J. F.; Gudiksen, M. S.; Duan, X. F.; Cui, Y.; Lieber, C. M. *Science* **2001**, *293*, 1455.
(13) Yu, S. H.; Antonietti, M.; Cöffen, H.; Giersig, M. *Angew. Chem. Int. Ed.* **2002**, *41*, 2356.
(14) Liao, H. W.; Wang, Y. F.; Liu, X. M.; Li, Y. D.; Qian, Y. T. *Chem. Mater.* **2000**, *12*, 2819.
(15) Chen, S. J.; Chen, X. T.; Xue, Z. L.; Zhou, J. H.; Li, J.; Hong, J. M.; You, X. Z. *J. Mater. Chem.* **2003**, *13*, 1132.
(16) Shi, H. T.; Qi, L. M.; Ma, J. M.; Cheng, H. M. *J. Am. Chem. Soc.* **2003**, *125*, 3450.
(17) Shi, H. T.; Qi, L. M.; Ma, J. M.; Cheng, H. M. *Chem. Commun.* **2002**, 704.
(18) Kwan, S.; Kim, F.; Akana, J.; Yang, P. D. *Chem. Commun.* **2001**, 447.
(19) Xie, B.; Wu, Y.; Jiang, Y.; Li, F. Q.; Wu, J.; Yuan, S. W.; Yu, W. C.; Qian, Y. T. *J. Cryst. Growth* **2002**, *235*, 283.
(20) Chen, S. J.; Zhou, J. H.; Chen, X. T.; Li, J.; Li, L. H.; Hong, J. M.; Xue, Z. L.; You, X. Z. *Chem. Phys. Lett.* **2003**, *375*, 185.
(21) Kobayashi, M.; Ishii, M.; Usuki, Y. *Nucl. Instrum. Methods Phys. Res., Sect. A* **1998**, *406*, 442.
(22) Hara, K.; Ishii, M.; Kobayashi, M.; Nikl, M.; Takano, H.; Tanaka, M.; Tanji, K.; Usuki, Y. *Nucl. Instrum. Methods Phys. Res., Sect. A* **1998**, *414*, 325.

10.1021/la035578b CCC: $27.50
Published on Web 01/06/2004

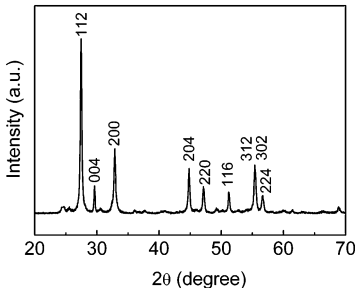

Figure 1. XRD pattern of the as-prepared sample 1.

gation, washed with distilled water and absolute ethanol several times, and dried in a vacuum at 60 °C for 4 h.

The crystallinity and phase purity of the products were examined by powder X-ray diffraction (XRD) with a Rigaku D/max 2550V X-ray diffractometer using graphite-monochromatized high-intensity Cu Kα radiation ($\lambda = 1.541\ 78$ Å). The morphology of the products was characterized by transmission electron microscopy (TEM, JEOL JEM-200CX, using an accelerating voltage of 200 kV). Samples were deposited on thin amorphous carbon films supported by copper grids from ultrasonically processed ethanol solutions of the products.

Results and Discussion

Figure 1 shows the typical XRD pattern of sample 1 that was aged in the mother solution at room temperature for 1 h. All the reflections of the XRD pattern can be indexed to a pure tetragonal phase [space group: $I4_1/a$ (No. 88)] of $PbWO_4$ with lattice constants $a = 5.443$ Å and $c = 12.054$ Å, which are in good agreement with the reported data ($a = 5.445$ Å, $c = 12.050$ Å, JCPDS File no. 85-1857). Sample 2, which was aged in the mother solution at room temperature for 6 h, and sample 3, which was crystallized at 160 °C for 20 h via a hydrothermal route, have similar XRD patterns to that of sample 1, as shown in Figure 1. These XRD patterns indicate that well-crystallized $PbWO_4$ crystals can be easily obtained under the current synthetic conditions. The yield of $PbWO_4$ nano- and microcrystals produced by this method is reproducibly higher than 95%.

The morphologies and microstructures of the as-prepared samples were further investigated with TEM and selected-area electron diffraction (SAED). As shown in Figure 2, these samples prepared under different conditions display the interesting morphologies of rods, spindles, and pagodas, respectively. Figure 2a shows the TEM micrograph for sample 1, from which one can see that the nano- and microstructured $PbWO_4$ crystals display rodlike morphology with diameters of 80−500 nm and lengths of 0.5−2 μm. The SAED pattern (inset in Figure 2a), taken from a randomly chosen single rod, shows that it is crystalline and exhibits discontinuous rings rather than full rings, indicating that it could consist of $PbWO_4$ polycrystals with an oriented crystallographic axis. Figure 2b shows the morphology of as-prepared $PbWO_4$ microcrystals for sample 2. With the aging time increasing from 1 to 6 h for the mother solution, the $PbWO_4$ crystals changed from nano- and microrods (shown in Figure 2a) to be of a conical tip and had formed spindles with lengths of the major axis ranging from ∼1 to ∼3 μm and lengths of the minor axis in the range 0.5−0.8 μm. The corresponding SAED pattern taken from a randomly chosen single spindle by focusing the electron beam along the [4 −10 1] direction is shown in the inset of Figure 2b. It can be indexed as the reflections of the tetragonal $PbWO_4$ structure, which is consistent with the result obtained from XRD. Electron diffraction patterns taken from different regions of this individual spindle are the same. Such homogeneity in the crystalline structure implies that $PbWO_4$ microspindles synthesized using the present procedure are single-crystalline in structure.

It is very interesting that the pagodas with ordinal layers and decrescent diameters were also observed, as shown in Figure 2c,d. $PbWO_4$ obtained via hydrothermal crystallization at 160 °C for 20 h (sample 3) had grown into pagodalike microcrystals with lengths of 0.8−1.5 μm and top diameters of 60−110 nm. The SAED pattern (inset of Figure 2d), taken from a single pagoda by focusing the electron beam along the [6 −4 1] direction, shows the single-crystalline nature and can also be indexed to the reflections of tetragonal $PbWO_4$ structure. Electron diffraction patterns taken from different regions of this individual pagoda are the same.

The morphology and dimensions of the products were also found to be strongly dependent on other reaction conditions such as the initial concentration of Na_2WO_4 and $Pb(CH_3COO)_2$, the reactant supply rate, and the molar ratio between the repeating unit of PVP and Na_2WO_4 [or $Pb(CH_3COO)_2$]. For example, when the initial concentration of Na_2WO_4 [or $Pb(CH_3COO)_2$] was increased to 0.2 mol L^{-1} or above, the products were dominated by microparticles with irregular shapes. With the increase of the reactant supply rate in the range of 0.05−0.30 mL min^{-1}, the size of the products became larger. However, if the reactants were rapidly added within several seconds through a direct mixing of reactants at room temperature without using the three-channel injection technique, the major morphologies were large aggregates of irregularly shaped microstructures. When the molar ratio between the repeating unit of PVP and Na_2WO_4 [or $Pb(CH_3COO)_2$] was varied in the range of 1−3, no obvious morphology change was observed. However, if the molar ratio was reduced to 0.5 or increased to 6, the size and morphology of the products became nonuniform. Therefore, the size or morphology of $PbWO_4$ crystals can be tuned easily by controlling the experimental conditions.

In the reaction process, $PbWO_4$ nuclei were generated via the reaction between Pb^{2+} and WO_4^{2-} in the solution. The freshly formed nuclei of $PbWO_4$ have a strong tendency to grow into larger particles. Especially, the controlled reactant supply rate by the three-channel injection technique under stirring plays a crucial role on the formations of $PbWO_4$ nano- and microcrystals, which maintains the amount of $PbWO_4$ nuclei in the solution and controls the crystal growth rate. In addition, the use of coordination reagent (polymeric or monomeric) to control the morphological evolution of nanostructures in the solution phase had been extensively explored in previous studies.[23] It is generally accepted that the coordination reagent kinetically controls the growth rates of various faces of nanocrystals through selective adsorption and desorption on these surfaces.[4,24] There seems to be a selectivity between the $PbWO_4$ crystal surfaces and the functional groups of the coordination reagent. Moreover, PVP in our experimental procedures may serve as a stabilizer, which inhibits $PbWO_4$ particles from aggregating. After continuous nucleation and growth for 6 h, spindlelike $PbWO_4$ crystals (sample 2) evolved from rodlike $PbWO_4$ polycrystals (sample 1). This phenomenon may be explained by the Ostwald ripening process, in which crystal growth is described in terms of growth of larger particles at the expense of smaller particles. Reduction in surface energy is the primary driving force for crystal

(23) Roosen, A. R.; Carter, W. C. *Physica A* **1998**, *261*, 232.
(24) Sun, Y. G.; Xia, Y. N. *Adv. Mater.* **2002**, *14*, 833.

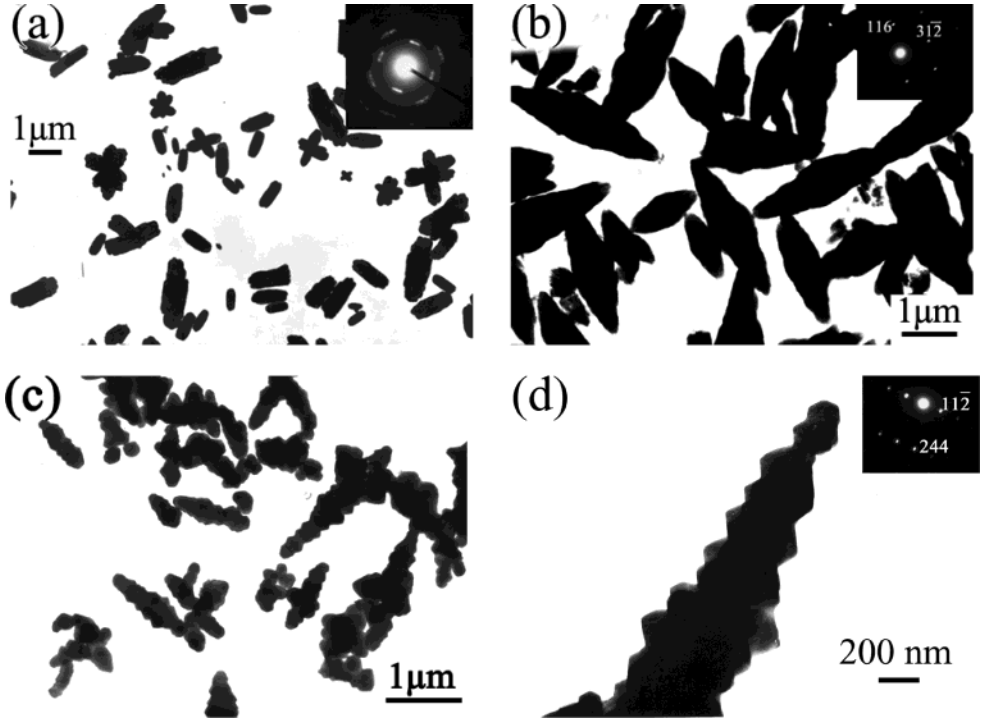

Figure 2. TEM images of the samples obtained under different conditions: (a) sample 1, the same sample as in Figure 1, aged at room temperature for 1 h after terminating the reactant supply; (b) sample 2, aged at room temperature for 6 h after terminating the reactant supply; (c) sample 3, hydrothermally crystallized at 160 °C for 20 h after terminating the reactant supply; and (d) magnified image of a single $PbWO_4$ pagoda from sample 3. Each inset shows the corresponding SAED pattern.

growth and morphology evolution.[25] After the hydrothermal crystallization at 160 °C for 20 h, pagodalike $PbWO_4$ crystals (sample 3) evolved, which may follow the oriented attachment mechanism proposed by Penn and Benfield.[25] The oriented attachment mechanism involves crystal growth by addition of solid crystals to the specific surfaces. This occurs in a precise, crystallographically controlled manner, resulting in coherent interfaces and leading to the development of single-crystalline $PbWO_4$ pagodas. The synthetic approach described in this paper may also be extended to the synthesis of other kinds of nanostructured materials.

In summary, we have developed a new route for the morphology-controlled synthesis of $PbWO_4$ nano- and microcrystals. The yield of $PbWO_4$ crystals is reproducibly higher than 95%. It is a simple route that involves no seeds, catalysts, or templates and is very promising for the low-cost and large-scale production of $PbWO_4$ nano- and microcrystals with various morphologies. The growth mechanism and properties of rodlike, spindlelike, and pagodalike $PbWO_4$ nano- and microcrystals are worth further study, and related research is in progress. These $PbWO_4$ nano- and microcrystals with various morphologies may find their applications in a variety of areas such as catalysis, electronics, photonics, photochemistry, and so on.

Acknowledgment. Financial support from Chinese Academy of Sciences (CAS) under the Program for Recruiting Outstanding Overseas Chinese (Hundred Talents Program) is gratefully acknowledged. We thank the Innovation Research Fund from Shanghai Institute of Ceramics, Chinese Academy of Sciences.

LA035578B

(25) Penn, R. L.; Banfield, J. F. *Geochem. Cosmochim. Acta* **1999**, *63*, 1549.